


# 2,5-dimethylcelecoxib improves immune microenvironment of hepatocellular carcinoma by promoting ubiquitination of HBx-induced PD-L1

Zhanfei Chen,<sup>1</sup> Yiyin Chen,<sup>1</sup> Lirong Peng,<sup>1</sup> Xiaoqian Wang,<sup>1</sup> Nanhong Tang <sup>1,2,3</sup>

**To cite:** Chen Z, Chen Y, Peng L, *et al.* 2,5-dimethylcelecoxib improves immune microenvironment of hepatocellular carcinoma by promoting ubiquitination of HBx-induced PD-L1. *Journal for ImmunoTherapy of Cancer* 2020;8:e001377. doi:10.1136/jitc-2020-001377

► Additional material is published online only. To view please visit the journal online (<http://dx.doi.org/10.1136/jitc-2020-001377>).

Accepted 10 September 2020



© Author(s) (or their employer(s)) 2020. Re-use permitted under CC BY-NC. No commercial re-use. See rights and permissions. Published by BMJ.

<sup>1</sup>Department of Hepatobiliary Surgery and Fujian Institute of Hepatobiliary Surgery, Fujian Medical University Union Hospital, Fuzhou, China

<sup>2</sup>Fujian Medical University Cancer Center, Fujian Medical University, Fuzhou, China

<sup>3</sup>Key Laboratory of Ministry of Education for Gastrointestinal Cancer, Fujian Medical University, Fuzhou, China

**Correspondence to**  
Professor Nanhong Tang;  
fztnh@fjmu.edu.cn

## ABSTRACT

**Background** 2,5-dimethylcelecoxib (DMC) is a targeted inhibitor of microsomal prostaglandin E synthase-1 (mPGES-1), a key enzyme in the PGE2 synthesis pathway of inflammatory mediators. Previous studies have confirmed that DMC can inhibit the growth of hepatitis B virus (HBV)-related hepatocellular carcinoma (HCC). However, it is not known whether DMC is involved in the changes of tumor immune microenvironment.

**Methods** In this study, we explored the effects of DMC on HBV-related HCC immune microenvironment, and deeply analyzed its unique effect and mechanism on programmed death receptor 1 (PD-1) and its ligand 1 (PD-L1) pathway.

**Results** Clinical hepatoma tissues detection showed that compared with non-virus-related HCC, the level of CD8 of HBV-related HCC was significantly lower, while the levels of PD-L1 and CD163 were higher. In vivo experiments indicated that DMC could increase the level of tumor infiltrating CD8<sup>+</sup> T cells in hepatitis B virus X (HBx) (+) hepatoma cells implanted mouse models, and inhibit the expression of PD-L1 and CD163 in tumor tissues. DMC combined with atezolizumab had more significant antitumor effect and stronger blocking effect on PD-1/PD-L1 pathway. Mechanism studies have shown that DMC can promote ubiquitin degradation of HBx-induced PD-L1 protein in HCC cells by activating adenosine 5'-monophosphate-activated protein kinase pathway. Further experiments confirmed that this process was mainly mediated by E3 ligase RBX1.

**Conclusions** Our results uncover a role for DMC in promoting HBV-related HCC immune microenvironment, which not only enrich the relationship between inflammatory factors (mPGES-1/PGE2 pathway) and immunosuppression (PD-L1), but also provide an important strategic reference for multitarget or combined immunotherapy of HBV-related HCC.

## BACKGROUND

The therapeutic effect of hepatitis B virus (HBV) related inflammation and tumor is highly related to the persistent function of effector T cells in vivo. Immune cells, especially CD8<sup>+</sup> T cells, are the key factors in controlling HBV replication.<sup>1</sup> However, HBV-related hepatocellular carcinoma (HCC) microenvironment has more obvious

characteristics of immunosuppression and T cell failure than non-virus-related HCC.<sup>2</sup> Studies have confirmed that a variety of mechanisms are closely related to HBV-specific T cells dysfunction: persistent high viral load and high antigen levels, inhibitory cytokines, dendritic cell and regulatory T cell.<sup>3</sup> There are a number of strategies to restore failure-specific T cells, including blocking the interaction of inhibitory receptors, changing the availability of activated and inhibitory cytokines, molecular reprogramming of failed T cells and so on.<sup>4</sup> Programmed death receptor 1 (PD-1) is the main and key inhibitory receptor.<sup>5</sup> Immunotherapy aimed at blocking PD-1 and its ligand 1 (PD-L1) has become a valuable means to cure tumors.<sup>6</sup> Due to the complexity of the immune environment caused by viral infection, the blocking of single receptor can not get the ideal effect, and it will also cause immune-related adverse events (irAEs).<sup>7</sup> Therefore, combination therapy or multitarget effect may be a more effective strategy for HBV-related HCC.<sup>8</sup>

Prostaglandin E2 (PGE2) is an important inflammatory mediator associated with HBV infection. PGE2 can also participate in the immune response as an immunosuppressive factor<sup>9</sup> and accelerate the senescence of CD8<sup>+</sup> T cells in a variety of tumors.<sup>10</sup> Xu *et al.*<sup>11</sup> found that hepatic stellate cells can induce myeloid-derived suppressor cells aggregation and activation through PGE2 in HCC, which suppresses immune factors in the microenvironment. Microsomal prostaglandin E synthase-1 (mPGES-1) is the terminal rate-limiting enzyme of the inflammatory mediator PGE2, which is only induced by inflammatory stimulation.<sup>12</sup> The expression of mPGES-1 increased step by step in atypical hyperplastic nodules, well differentiated, moderately differentiated and poorly differentiated HCC groups.<sup>13</sup> Downregulation of mPGES-1 can

reduce the invasion and metastasis potential of HCC.<sup>14</sup> Previous studies of our group have found that hepatitis B virus X (HBx) can upregulate the expression of mPGES-1 through transcription factor EGR1, and then increase the secretion of PGE2.<sup>15,16</sup> However, the relationship between mPGES-1 and HBV-related HCC immune microenvironment is still unknown.

2,5-dimethylcelecoxib (DMC) could effectively inhibit the expression of mPGES-1 and reduce the secretion of PGE2. It has been found that DMC is superior to celecoxib in anti-inflammatory and antitumor aspects while lacking COX enzyme inhibitory activity in a variety of tumors.<sup>17,18</sup> PGE2 is closely related to immune microenvironment, so DMC also has the function of improving the immunosuppressive state of HBV related HCC. However, what is the overall effect of DMC on HBV-related HCC immune microenvironment? Does it also have the function of regulating the expression of immune checkpoint molecules? In particular, does it have a unique effect on the PD-1/PD-L1 pathway? None of these meaningful problems have been solved. Thus, this study intends to study the relationship between HBV infection factor (HBx) and tumor immune microenvironment (CD8, PD-L1 and CD163) from clinical HCC tissue samples, and then to further explore the ability of DMC inhibiting tumor proliferation in the implanted tumor mice models of HBx (+) liver cancer cells, as well as its influence on tumor immune microenvironment. Finally, the special mechanism of the effect of DMC on the immune function of HBV-related HCC was clarified by cytological experiments. Our study provides a new strategy for combined or multitarget immunotherapy of HBV-related HCC.

## METHODS

### Patients and tissue samples

Human HCC tissue samples were collected from patients who underwent surgery in the Fujian Medical University Union Hospital from January 2009 to December 2010. In this study, there were 40 patients, all of them were histologically confirmed as primary hepatic carcinoma, and did not receive any radiotherapy and chemotherapy before operation, and the informed consent was obtained before the sample collection. The staging of each patient was evaluated according to the American Joint Committee on Cancer version 8 (AJCC8).

### Induction of HCC in mice

Male C57BL/6 mice aged 4–6 weeks were subcutaneously inoculated with  $1 \times 10^7$  mouse hepatoma cells Hepa1-6/HBx or Hepa1-6/Vec on the right side to establish the mouse hepatoma model. Five days after implantation, when the tumor grew to 60 mm<sup>3</sup>, it was divided into several groups with five mice in each group. Intraperitoneal injection of DMC, or atezolizumab (an anti-PD-L1 monoclonal antibody, has been approved by FDA for clinical use,<sup>19</sup> or DMC+atezolizumab, or control (1% Dimethyl Sulfoxide-Phosphate Buffer Saline, DMSO-PBS). DMC

was treated once a day (10 mg/kg each time) for a total of 7 times. Atezolizumab was treated every other day (5 mg/kg each time) for four times. The volume of tumor was measured every other day. 24 hours after the last injection, the model mice were put into CO<sub>2</sub> box and killed. The number and distribution of tumor infiltrating macrophages and CD8<sup>+</sup> T lymphocytes were detected by immunohistochemistry. The tumor cells were detected by flow cytometry with fluorescence labeling.

Other materials and methods are available in online supplemental file 1 and online supplemental file 2.

## RESULTS

### Pathological features of clinical patients with primary hepatic carcinoma

The clinicopathological features of 40 patients with primary hepatic carcinoma were as follows (table 1): the median age was 62.5 years (range 34–86). In the tumor, node, metastases, stage I–II accounts for 65.0%, and only one of the cases of stage III–IV (35.0%) was stage IV. According to the results of HBsAg detection, all samples were divided into HBV positive HCC and HBV negative HCC.

### Immune status of tumor microenvironment in patients with HBV-related HCC

HBx is one of the iconic proteins in patients with HBV infection. In order to show the expression level of HBx in 40 cases of HCC, we performed immunohistochemical detection on all samples. HBV negative HCC (15 cases) did not or low expression of HBx (mean optical density (MOD)=0.2626±0.05683), while HBx was obviously highly expressed (MOD=11.86±0.8189) in HBV positive HCC (25 cases) (figure 1A,B). Based on the above results, all clinical HCC tissues were divided into HBx positive group and HBx negative group. The difference of CD8 and PD-L1 expression between the two groups was also detected. In the HBx positive group, the CD8 expression decreased significantly (MOD=0.6424±0.05925), while in the HBx negative group, the immersion CD8 level was higher (MOD=6.221±1.071) (figure 1C,D). On the contrary, the expression of PD-L1 in the HBx positive group (MOD=5.566±0.5511) was significantly higher than that in the HBx negative group (MOD=0.5210±0.1034) (figure 1E,F). In addition, the level of PD-L1 in HBx positive group was increased not only in tumor cells (figure 1), but also in some immune cells (online supplemental figure S1). Based on the results, we speculated that HBx may enhance PD-1/PD-L1 signal pathway by promoting the expression of PD-L1 in tumor microenvironment, thus reduce the level of CD8<sup>+</sup> T cell infiltration and promoting tumor immune escape.

We compared the relationship between the expression of CD8 and PD-L1 with several important clinicopathological features affecting the occurrence and development of HCC (table 1). The expression of CD8 and PD-L1 was only closely related to HBV infection (p<0.001).

**Table 1** Clinicopathological characteristics of primary hepatic carcinoma patients

Characteristics	n	Tumor HBx expression			Tumor CD8 expression			Tumor PD-L1 expression		
		Low	High	P value	Low	High	P value	Low	High	P value
All patients	40 (100%)	15	25		30	10		24	16	
Gender										
Male	32 (80.0%)	12	20	1.000	25	7	0.361	18	14	0.333
Female	8 (20.0%)	3	5		5	3		6	2	
Age										
≤50	13 (32.5%)	4	9	0.542	11	2	0.330	10	3	0.130
>50	27 (67.5%)	11	16		19	8		14	13	
Tumor site										
Left	14 (35.0%)	6	8	0.608	9	5	0.251	8	6	0.787
Right	26 (65.0%)	9	17		21	5		16	10	
Tumor size										
≤5 cm	26 (65.0%)	9	17	0.608	21	5	0.251	14	12	0.279
>5 cm	14 (35.0%)	6	8		9	5		10	4	
HBV infection										
Positive	25 (62.5%)	0	25	<0.001	25	0	<0.001	9	16	<0.001
Negative	15 (37.5%)	15	0		5	10		15	0	
Pathological type										
Hepatocellular carcinoma	36 (90.0%)	13	23	0.586	28	8	0.224	22	14	0.667
Non-hepatocellular carcinoma	4 (10.0%)	2	2		2	2		2	2	
Pathological grading										
I-II	37 (92.5%)	13	24	0.278	27	10	0.299	22	15	0.806
III	3 (7.5%)	2	1		3	0		2	1	
TNM stage										
I-II	26 (65.0%)	9	17	0.608	21	5	0.251	14	12	0.279
III-IV	14 (35.0%)	6	8		9	5		10	4	

The difference between the positive group and the negative group was statistically significant ( $P < 0.001$ ).

HBV, hepatitis B virus; HBx, hepatitis B virus X; PD-L1, programmed death receptor 1 and its ligand 1; TNM, tumor, node, metastases.

CD163 and PD-L1 are both key indicators to reflect the immunosuppressive state of tumor microenvironment. We sought to study the correlation between them in HBV positive HCC. 15 cases of clinical HBV positive HCC were randomly selected and detected. The analysis revealed that there was a high positive correlation between the two proteins (figure 1G,H) (performance test of power=0.93095). This was consistent with the positive correlation between CD163 and CD274 gene expression in Gene Expression Profiling Interactive Analysis (GEPIA) database (online supplemental figure S2), so we think that compared with HBV-negative HCC, CD163 was also a higher level in HBV-positive HCC. In summary, the high expression of PD-L1 and CD163 proved the fact of immunosuppression in HBV positive HCC microenvironment.

### DMC can effectively inhibit the tumor growth of mice implanted with HBx (+) hepatoma cells

In previous study, we used mPGES-1 reporter cells to screen the effective mPGES-1 inhibitor DMC.<sup>12</sup> In order to explore the intervention effect of DMC on tumor immune microenvironment in vivo, we established HBx (+) hepatoma cells implanted mouse model and the mice were injected drug intraperitoneally (figure 2A). The results showed that compared with control group, tumor growth was significantly inhibited in DMC or atezolizumab groups, and more significant in combination with DMC and atezolizumab groups (figure 2B-D). At the same time, the expression of CD8, CD163 and PD-L1 were detected. Consistently, compared with control group, DMC or atezolizumab alone could increase the level of CD8<sup>+</sup> T cells infiltration and decrease the expression of

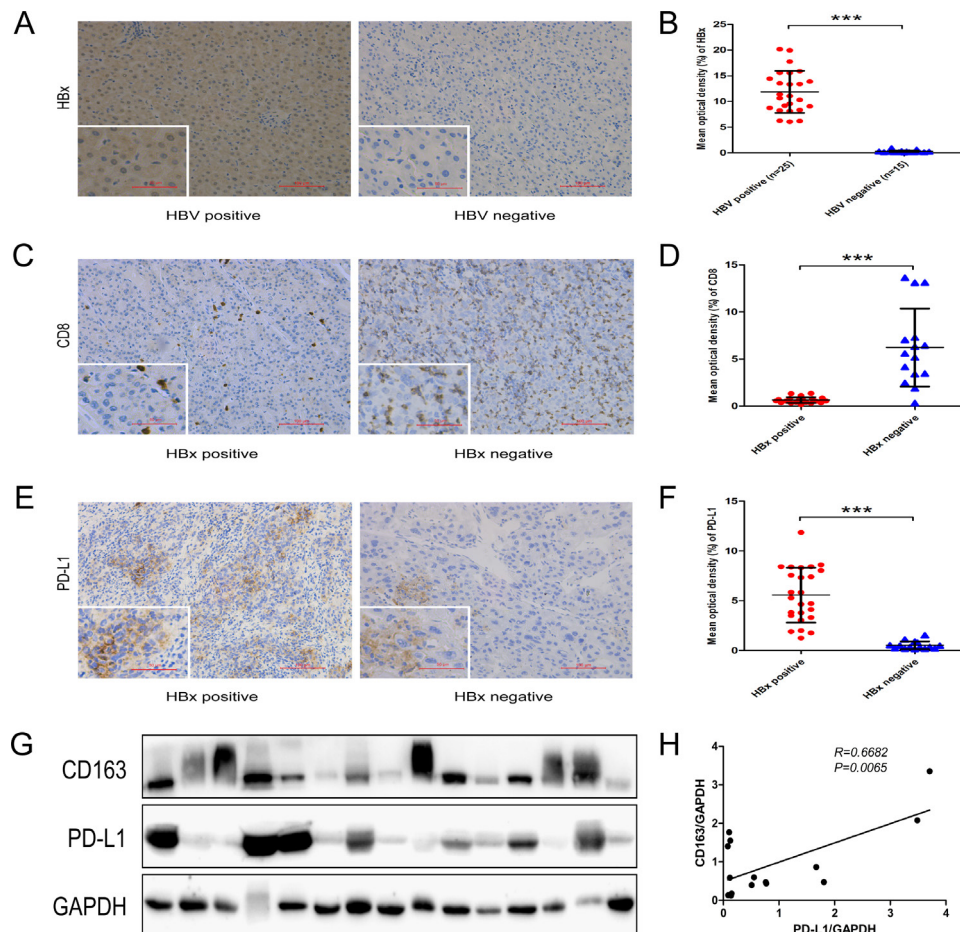


**Figure 1** Immune status of tumor microenvironment in patients with HBV-related HCC. (A–F) The expression of HBx (A), CD8 (C) and PD-L1 (E) were detected by immunohistochemistry in clinical samples (200 $\times$ ). The bottom left corner of each histochemical picture was a magnification representative field (400 $\times$ ). The semi-quantitative analysis of the results of HBx (B), CD8 (D) and PD-L1 (F), immunohistochemistry were expressed by the mean optical density. (G) The expression of CD163 and PD-L1 were detected in 15 HBV positive HCC patients. Glyceraldehyde-3-phosphate dehydrogenase (GAPDH) was used as the internal reference. (H) All the gray values of (G) were normalized by GAPDH internal reference, and the obtained data were made into the expression correlation map of PD-L1 and CD163. The  $r$  value and  $p$  value were analyzed (\*\* $p < 0.001$ ). HBx, hepatitis B virus X; HBV, hepatitis B virus; HCC, hepatocellular carcinoma; PD-L1, programmed death receptor 1 and its ligand 1.

PD-L1 and CD163, while the effect of combined DMC and atezolizumab group was more significant (figure 2E,F). Based on the results, we concluded that DMC can inhibit the expression of PD-L1 and show a more efficient ability to block PD-1/PD-L1 signals in combination with atezolizumab in vivo.

However, the result which was different from the expected was that in the control group of HBx (+) hepatoma mice, the infiltrating CD8<sup>+</sup> T cells also showed a higher level, which we speculated to be the results of HBx-induced acute immune stress in C57BL/6 mice.<sup>20</sup> In order to eliminate the interference of this factor on the results of figure 2E, we established an implanted tumor model of Hepa1-6/Vec (not expressing HBx) hepatoma cells, and the administration process was the same as that of the previous (figure 2A). We observed that DMC and atezolizumab alone still significantly inhibited tumor growth, while the combination group also showed a more significant inhibitory effect (figure 3A–C). Importantly, flow cytometry analysis showed that DMC combined with

atezolizumab could effectively increase the level of CD8<sup>+</sup> T cell infiltration (figure 3D), and the results also showed that the combination of the two drugs could significantly decrease the levels of CD163 and PD-L1 than any single drug (figure 3E). This suggested that the increase of CD8<sup>+</sup> T cell level after DMC intervention was indeed due to the improvement of immune efficacy by DMC, rather than the acute stress of the immune system to HBx factor. To sum up, DMC combined with atezolizumab can significantly improve the immune microenvironment and effectively inhibit the growth of HBx (+) liver tumors.

#### DMC improved the immune microenvironment of the coculture system of hepatoma cells overexpressing HBx and Peripheral blood mononuclear cells (PBMCs)

We further carried out in vitro experiments to verify the effect of DMC on the expression of PD-L1 in hepatoma cells overexpressing HBx. When the concentration of DMC was higher than 20  $\mu$ M, the inhibitory effect of DMC on the proliferation of HepG2 hepatoma cells

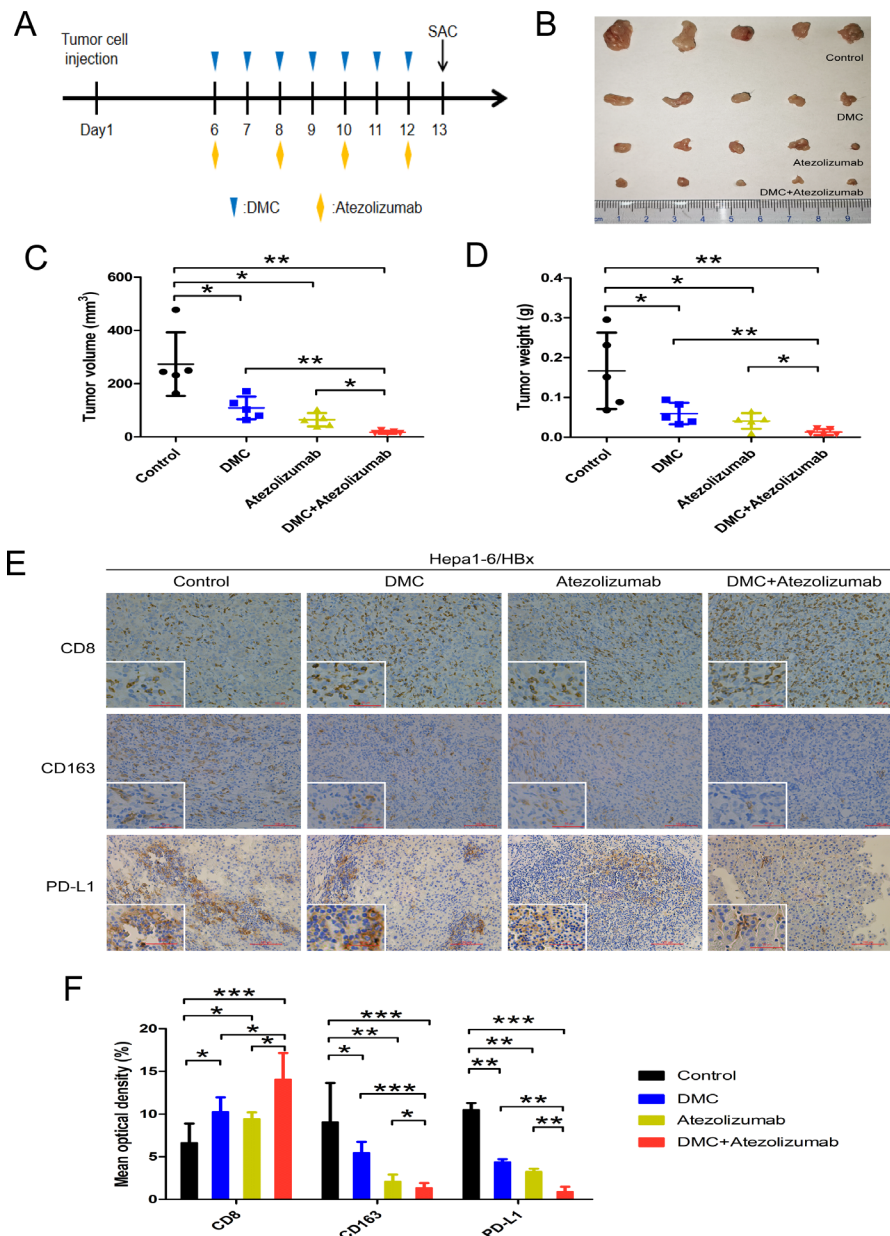


**Figure 2** DMC can effectively inhibit the tumor growth of HBx (+) hepatoma cells implanted mouse model. (A) Establishment and administration process of HBx (+) hepatoma cells implanted mouse model. On the first day, Hepa1-6/HBx cells were injected subcutaneously with  $1 \times 10^7$  million cells per mouse. On the sixth day, the drug was injected intraperitoneally. 24 hours after the last administration (day 12), the model mice were put into the carbon dioxide box and sacrificed, and the implanted tumor was taken (day 13). (B) Photos taken after the tumor were removed. (C) The volume of the tumor was measured on the day before the model mice were sacrificed. The mean  $\pm$ SD values of tumor volume in each group were as follows: control group:  $273.4 \pm 53.39 \text{ mm}^3$ , DMC group:  $109.2 \pm 19.04 \text{ mm}^3$ , atezolizumab group:  $64.84 \pm 11.19 \text{ mm}^3$ , combination group:  $17.77 \pm 2.255 \text{ mm}^3$ . (D) The weight was weighed after the tumor removal. The mean  $\pm$ SD values of the tumor weight of each group were as follows: control group:  $0.1666 \pm 0.04288 \text{ g}$ , DMC group:  $0.0596 \pm 0.01206 \text{ g}$ , atezolizumab group:  $0.0408 \pm 0.008840 \text{ g}$ , combination group:  $0.0130 \pm 0.003302 \text{ g}$ . (E) The expression of CD8, CD163 and PD-L1 proteins of the four groups were detected by immunohistochemistry (200 $\times$ ). The bottom left corner of each histochemical picture was a magnification representative field (400 $\times$ ). (F) Took pictures under 200 $\times$  microscope visual field. There were five tumor specimens in each group. All the MOD values were drawn into a histogram for statistical analysis (\* $p < 0.05$ , \*\* $p < 0.01$ , \*\*\* $p < 0.001$ ). DMC, 2,5-dimethylcelecoxib; HBx, hepatitis B virus X; PD-L1, programmed death receptor 1 and its ligand 1.

was stronger (figure 4A). When DMC was higher than  $12.5 \mu\text{M}$ , the proliferation of Huh7 hepatoma cells was gradually inhibited (figure 4B). Then, we constructed the coculture system of hepatoma cells overexpressing HBx and PBMCs, and added the concentration of

DMC that did not affect cell proliferation (HepG2:  $10 \mu\text{M}$ ; Huh7:  $10 \mu\text{M}$ ), and then extracted tumor cells and PBMCs for analysis. The results showed that: (1) in figure 4C,D, HBx promoted the expression of PD-L1 in two hepatoma cells. And PD-L1 expression was

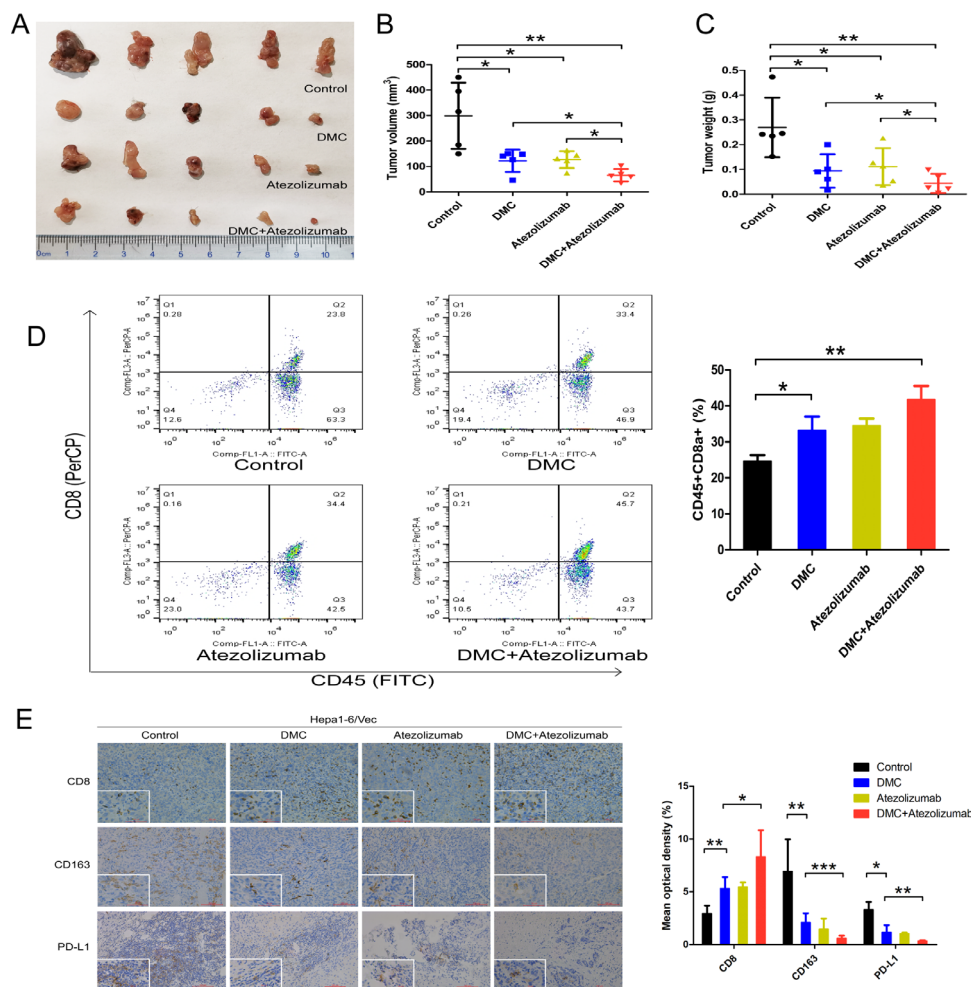


**Figure 3** DMC can effectively inhibit the growth of tumor in mice implanted with hepatoma cells. (A) Established C57BL/6 mouse hepatoma model by subcutaneous tumor formation of Hepa1-6/Vec cells. (B) The tumor volume of each group was measured and statistically analyzed before the model mice were sacrificed. The mean±SD values of the tumor volume of each group were as follows: control group:  $299.1 \pm 58.13 \text{ mm}^3$ , DMC group:  $122.3 \pm 19.56 \text{ mm}^3$ , atezolizumab group:  $127.2 \pm 14.86 \text{ mm}^3$ , combination group:  $65.40 \pm 10.94 \text{ mm}^3$ . (C) The weight of each group of was measured and statistically analyzed after the tumor removal. The mean±SD values of the tumor weight of each group were as follows: control group:  $0.2694 \pm 0.05374 \text{ g}$ , DMC group:  $0.0938 \pm 0.03026 \text{ g}$ , atezolizumab group:  $0.1116 \pm 0.03333 \text{ g}$ , combination group:  $0.0438 \pm 0.01719 \text{ g}$ . (D) Flow cytometry was used to detect the expression of CD8 in the fresh tumor samples. The double positive region of CD45 (Fluorescein isothiocyanate isomer, FITC) and CD8 were the required CD8<sup>+</sup> T cell region (Q2 region). The values of Q2 region were summarized into the bar chart on the right side. (E) The hepatoma model was established by Hepa1-6/Vec cells, and the expression of CD8, CD163 and PD-L1 proteins were detected (200×). The bottom left corner of each histochemical picture was a magnification representative field (400×). The mean optical density values were made into a bar chart (\* $p < 0.05$ , \*\* $p < 0.01$ , \*\*\* $p < 0.001$ ). DMC, 2,5-dimethylcelecoxib; PD-L1, programmed death receptor 1 and its ligand 1.

suppressed after DMC treatment. (2) The expression of HBx in hepatoma cells significantly decreased the level of CD8<sup>+</sup> T cells in PBMCs (from 38.1% to 26.5%) and increased the expression of PD-L1 in monocytes and macrophages (from 36.4% to 51.4%). More importantly, the intervention of DMC significantly increased the level of CD8<sup>+</sup> T cells (from 26.5% to 39.5%) and effectively inhibited the expression of PD-L1 in monocytes and macrophages (from 51.4% to 41.1%) (figure 4E,F). In summary, our data revealed that DMC can improve the level of CD8<sup>+</sup> T cells and inhibit the expression of PD-L1 in the coculture system of PBMCs and hepatoma cells overexpressing HBx.

### DMC inhibited HBx-induced PD-L1 protein expression in HCC cells by activating adenosine 5'-monophosphate-activated protein kinase

In order to explore the mechanism of DMC inhibiting the expression of PD-L1 in HCC cells in vitro. HepG2 cell was treated with DMC (10  $\mu\text{M}$ ) and analyzed by microarray. Then, all the differential genes (online supplemental figure S3) were selected for Gene Ontology (GO) and Kyoto Encyclopedia of Genes and Genomes (KEGG) analysis. Indeed, DMC treatment had a significant effect on the energy metabolism of tumor cells (figure 5A,B), in which adenosine 5'-monophosphate-activated protein kinase (AMPK) pathway might be involved (figure 5).

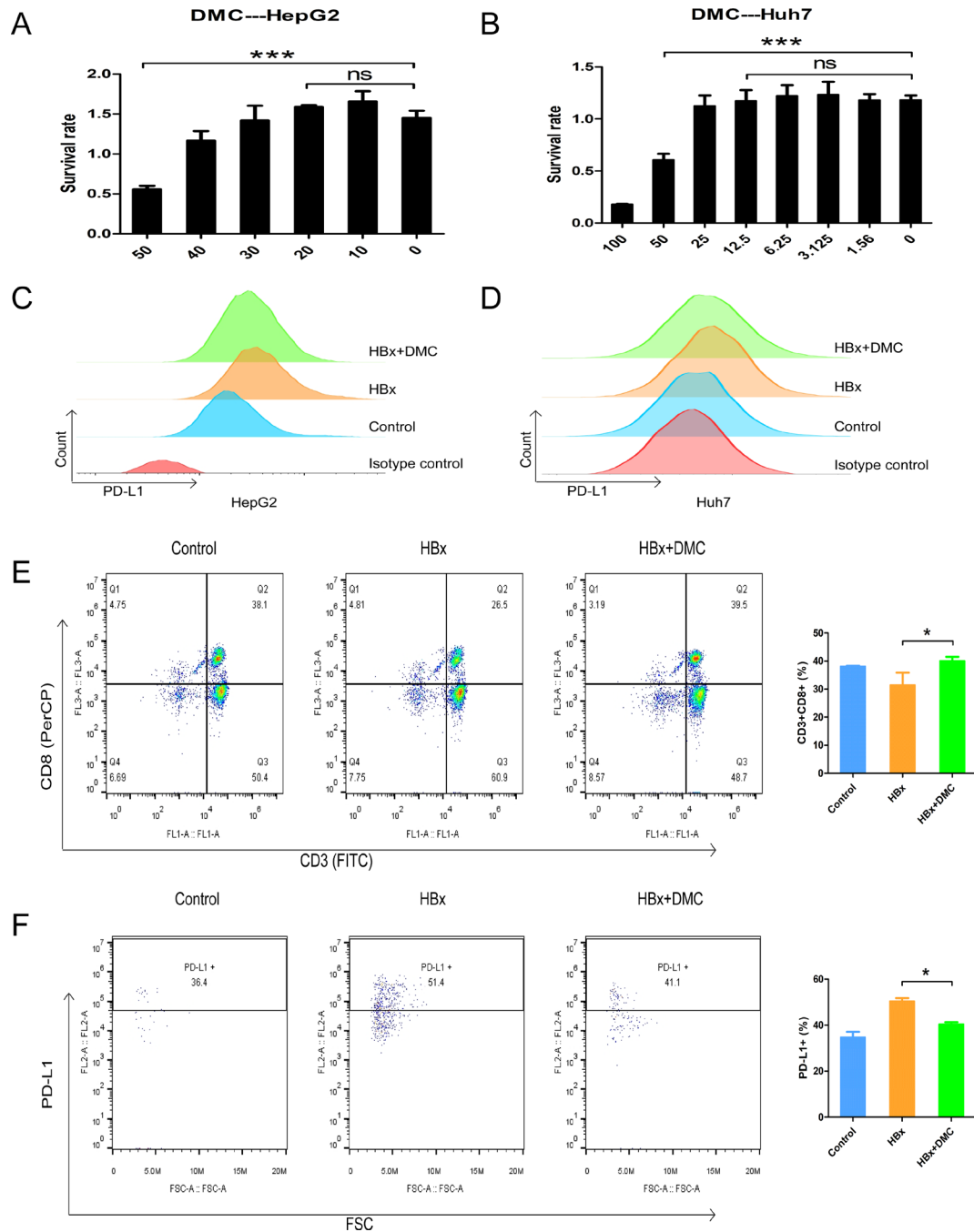


**Figure 4** DMC improved the immune microenvironment of the coculture system of hepatoma cells overexpressing HBx and PBMCs. (A–B) The inhibitory effect of DMC on the proliferation of HepG2 and Huh7 cells. (C–D) The tumor cells were extracted from the co-culture system of different groups, and the expression of PD-L1 protein was detected by flow cytometry. Isotype control was the homologous control group of the PD-L1 antibody, and the control group was the negative control (\* $p < 0.05$ , \*\* $p < 0.01$ , \*\*\* $p < 0.001$ ). (E) PBMCs cells from different groups of coculture systems were detected. The target cell group was recognized by CD3 and CD8 antibodies, and the double positive region (Q2 region, namely CD3<sup>+</sup> CD8<sup>+</sup>) were the required CD8<sup>+</sup> T cells. FITC and PerCP need to perform fluorescence compensation. The results of Q2 region were drawn as a bar chart on the right, the abscissa represented three different groups, and the ordinate represented the value of CD3<sup>+</sup>CD8<sup>+</sup> (%) (\* $p < 0.05$ ). (F) PBMCs cells were also extracted, and the expression of PD-L1 was detected after different intervention. After excluding the isotype control, the results of the PD-L1 positive area (PD-L1<sup>+</sup>) (monocytes and macrophages in PBMCs) were counted in the bar chart on the right, where the abscissa represents three different groups and the ordinate represents the PD-L1<sup>+</sup> (%) value (\* $p < 0.05$ ). DMC, 2,5-dimethylcelecoxib; FITC, fluorescein isothiocyanate isomer; FSC, forward scatter; HBx, hepatitis B virus X; PBMCs, peripheral blood mononuclear cells; PD-L1, programmed death receptor 1 and its ligand 1.

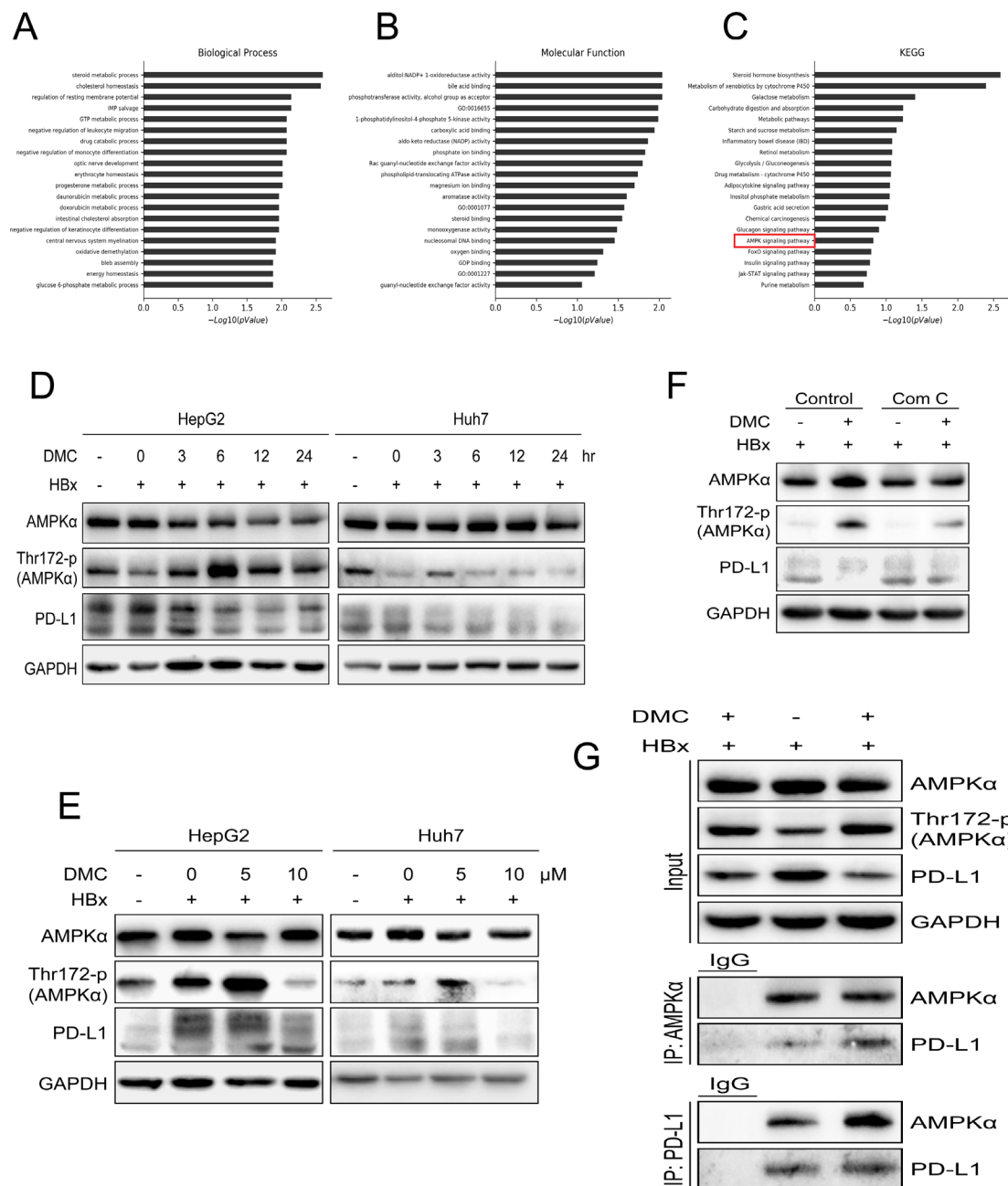


**Figure 5** DMC inhibited the expression of HBx-induced PD-L1 protein in hepatoma cells by activating adenosine 5'-monophosphate-activated protein kinase (AMPK) pathway. (A–C) In the results of microarray, all the differential genes were analyzed by Gene Ontology (GO) and Kyoto Encyclopedia of Genes and Genomes (KEGG) pathway analysis, which showed the enrichment of differential genes in biological processes, molecular functions and KEGG. (D) The effect of DMC on the expression of PD-L1 and AMPK $\alpha$  in hepatoma cells overexpressing HBx for different time. Hepatoma cells were transiently transfected with HBx plasmid (1  $\mu$ g/mL) for 24 hours, then DMC was added to intervene at different time points. Glyceraldehyde-3-phosphate dehydrogenase (GAPDH) was used as the internal control. (E) After the intervention of DMC with different concentrations for 24 hours, the expression of PD-L1 and AMPK $\alpha$  protein in hepatoma cells overexpressing HBx were affected. Hepatoma cells were transiently transfected with HBx plasmid (1  $\mu$ g/mL) for 24 hours, and then interfered with different concentrations of DMC for 24 hours. Similarly, the internal reference was GAPDH. (F) Hepatoma cells (HepG2) overexpressing HBx were treated with DMC for 24 hours. GAPDH was used as an internal control. AMPK inhibitor Compound C pretreated the cells for 4 hours before DMC intervention. (G) Co-IP was used to detect the interaction between AMPK $\alpha$  and PD-L1 protein after DMC treatment. DMC, 2,5-dimethylcelecoxib; HBx, hepatitis B virus X; PD-L1, programmed death receptor 1 and its ligand 1.

Next, we tried to explore the relationship between AMPK and PD-L1 expression after DMC treatment. (1) HepG2 and Huh7 cells with overexpression of HBx were treated with DMC for different times. Indeed, the

expression of PD-L1 in HepG2 and Huh7 cells increased induced by HBx. And with the extension of DMC intervention time, Thr172 AMPK $\alpha$  protein increased gradually and the expression of PD-L1 was inhibited continuously



(figure 5D). (2) Using the same method, different concentrations of DMC were used to treat the cells for 24 hours. With the increase of concentration, DMC significantly downregulated the level of PD-L1 induced by HBx in HepG2 and Huh7 cells (figure 5E). This suggested that DMC inhibited HBx-induced PD-L1 expression in HCC cells in a time-dependent and dose-dependent manner, meanwhile, DMC can activate AMPK pathway. We speculated that there was a relationship between the inhibition of PD-L1 expression and the activation of AMPK pathway. In order to verify this, we used Compound C (10  $\mu$ M) to block the activation of AMPK pathway in HepG2 cells. It was found that after blocking AMPK, the expression of HBx-induced PD-L1 protein inhibited by DMC was restored (figure 5F). More importantly, Co-IP assay showed that the interaction between AMPK $\alpha$  and PD-L1 protein was significantly enhanced after DMC treatment (figure 5G). In summary, our experimental data showed that DMC inhibits HBx-induced PD-L1 protein expression by activating AMPK pathway.

#### DMC leads to ubiquitin degradation of PD-L1 (HBx-induced) through the action of E3 ligase RBX1

In order to further investigate the mechanism of DMC inhibited the expression of PD-L1 after activating AMPK pathway in HCC cells, we detected the location relationship between PD-L1 and GRP94 (protein characterizing endoplasmic reticulum) at different time points. The amount of co-localization of PD-L1 and GRP94 proteins increased gradually after DMC treatment (figure 6A), indicating that DMC led to abnormal accumulation of PD-L1 in endoplasmic reticulum. Meanwhile, the inhibitory effect of DMC on PD-L1 protein band was similar to that of tunicamycin (an inhibitor of glycosylation) (figure 6B). These results suggested that the activation of AMPK by DMC may affect the normal synthesis of PD-L1 protein, resulting in abnormal accumulation and degradation in the endoplasmic reticulum.

Furthermore, the HepG2 cells overexpressing HBx were detected by IP-MS after DMC treatment (online supplemental figure S4A,B). KEGG analysis showed that “proteasome” and “protein processing in endoplasmic reticulum” (figure 6C and online supplemental figure S5) were found in the first three candidate pathways binding to PD-L1 protein. These results strongly proved that the abnormal accumulation of PD-L1 in the endoplasmic reticulum was indeed related to abnormal protein processing, and its degradation was related to the ubiquitin proteasome pathway. The protein analysis of IP-MS showed that 158 new proteins appeared after DMC treatment (online supplemental figure S6), from which we analyzed the protein related to the degradation of PD-L1 (figure 6D) and selected three candidate proteins: HSPH1, RBX1 and UBE2K (online supplemental figure S7A–C) to verify. The interaction between three candidate proteins with PD-L1 were significantly enhanced after DMC treatment (figure 6E). And the ubiquitination level of PD-L1 protein was significantly upregulated

(figure 6F), which was consistent with the results of mass spectrometry. RBX1, as an E3 ubiquitin ligase, plays an important role in the ubiquitin proteasome pathway.<sup>21</sup> In order to explain whether the ubiquitin of PD-L1 was related to RBX1, we used RBX1-siRNA to downregulate the expression of RBX1 in HepG2 cells. Notably, the ubiquitin level of PD-L1 was significantly downregulated with the intervention of RBX1-siRNA (figure 6G). The above data indicated that DMC leads to abnormal protein synthesis of PD-L1, and then ubiquitin degradation of PD-L1 was caused by the action of E3 ligase RBX1 (figure 7).

#### DISCUSSION

In this study, we found that the expression of PD-L1 in patients with HBV-related HCC was higher than that in patients with non-virus-related HCC, and the expression of CD8 was significantly lower in clinical HCC samples, which was consistent with the previously reported view that CD8<sup>+</sup> T cells were more functional failure in HBV-related HCC.<sup>2</sup> At the same time, this conclusion was also confirmed in the coculture cell system, that is, HBx promoted the PD-L1 expression of HCC cells and immune cells, and inhibited the level of CD8<sup>+</sup> T cells infiltration. With regard to the relationship among HBx, PD-L1 and CD8<sup>+</sup> T cells, some scholars believed that HBx upregulates the transcription level of B7-H1 gene through transcription factor NF- $\kappa$ B, which leads to the increase of PD-L1 protein expression and promotes T cells apoptosis.<sup>22</sup> Sun *et al*<sup>23</sup> proved that HBx can activate the transcriptional activity of B7-H1 through PTEN/ $\beta$ -catenin/c-Myc signal pathway and increase the expression of PD-L1, which can inhibit T cells response and promote HBV immune escape. These studies analyzed the mechanism of HBV factor affecting T cells function through PD-L1 from different signal pathways.

The complexity of HBV infection is bound to lead to multiple immunomodulatory mechanisms in the tumor microenvironment of HCC. In this study, we found the characteristics of the expression of another important immunosuppressive molecule CD163 (M2 macrophages) in HBV-related HCC tissues, indicating that the immune microenvironment immunosuppression caused by inflammatory factors of HBV infection is in many ways. In animal experiments, we found that the combination of DMC and atezolizumab showed stronger antitumor effect on HBx (+) hepatoma-bearing mice, indicating that DMC can play a better role in the inflammatory microenvironment of HBx (+). This effect was reflected not only in the effective improvement of immunosuppressive factors mediated by PD-L1, but also in the inhibitory effect on immunosuppressive cells dominated by M2 tumor-associated macrophages (TAM) cells. Some studies have shown that TAM can promote tumor occurrence and development by inhibiting antitumor immunity, promoting tumor angiogenesis and inducing tumor invasion and

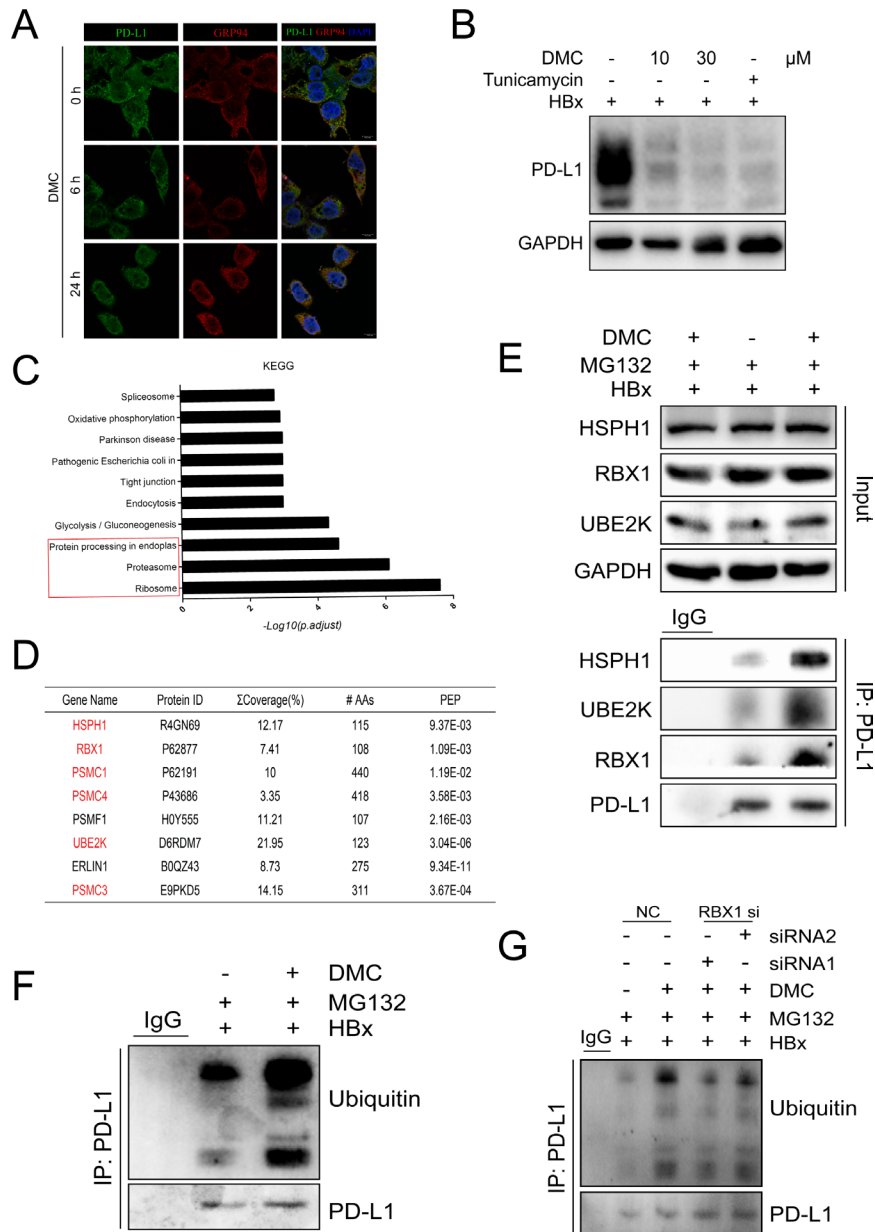


**Figure 6** DMC leads to ubiquitin degradation of PD-L1 (HBx-induced) through the action of E3 ligase RBX1. (A) The effect of DMC (10  $\mu\text{M}$ ) with different treatment time on the localization of PD-L1 protein in HepG2 cells overexpressing HBx. Green fluorescence was PD-L1 protein, red fluorescence was GRP94 protein and blue fluorescence was nucleus. The yellow fluorescence was where green and red overlap. (B) The detection of PD-L1 glycosylated protein caused by DMC. After transfection of HBx (1  $\mu\text{g}/\text{mL}$ ), HepG2 cells were treated with tunicamycin and DMC for 24 hours, respectively. GAPDH was the internal reference. (C) Analysis of the protein enrichment pathway in the mass spectrometry results, the red box in the picture was the first three enrichment pathways. (D) Analyzed the proteins related to the degradation process of PD-L1 protein from “158” for follow-up verification. (E) The expression of three candidate proteins were verified by western blot in the protein solution co-precipitated by PD-L1 antibody. In Input, GAPDH was the internal reference; in IP:PD-L1, PD-L1 was the internal reference. (F) The effect of DMC on the ubiquitination level of PD-L1 protein was detected by Ub antibody in the protein solution co-precipitated by PD-L1 antibody, and PD-L1 was used as the internal control. (G) To verify whether E3 ligase RBX1 was involved in the ubiquitin degradation of PD-L1 protein. HBx hepatoma cells treated with DMC (10  $\mu\text{M}$ ) were pretreated with two different sequences of RBX1-siRNA (siRNA1 and siRNA2), and the rescue of ubiquitin of PD-L1 was detected by co-immunoprecipitation. PD-L1 was the internal reference. DMC, 2,5-dimethylcelecoxib; GAPDH, glyceraldehyde-3-phosphate dehydrogenase; HBx, hepatitis B virus X; PD-L1, programmed death receptor 1 and its ligand 1.

metastasis. TAM infiltration is closely related to poor prognosis of patients.<sup>24</sup> Inhibiting the expression of M2 or promoting the transformation of M2 to M1 has become one of the main strategies of targeted TAM

therapy.<sup>25</sup> Although our results suggested that DMC can significantly downregulate the expression of CD163 in M2 TAM cells, due to the complexity of drug effects on immune microenvironment, there must be other

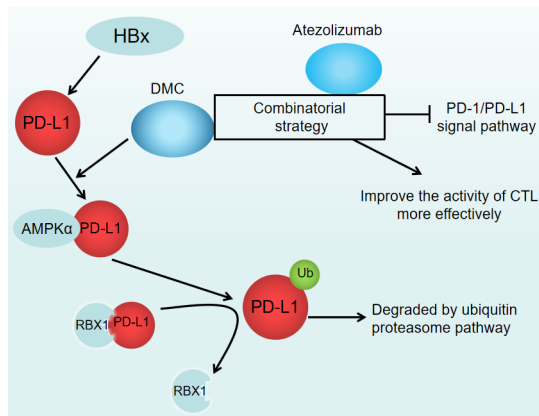


**Figure 7** DMC results in abnormal synthesis and ubiquitination of PD-L1 protein in HBx positive hepatoma cells. CTL, cytotoxic T lymphocyte; DMC, 2,5-dimethylcelecoxib; HBx, hepatitis B virus X; PD-1, programmed death receptor 1; PD-L1, PD-1 and its ligand 1.

regulatory relationships between DMC and TAM, which are worthy of our further study.

Microarray analysis and western blot showed that AMPK pathway was related to the inhibition of HBx-induced PD-L1 expression by DMC. AMPK is a sensor of cellular energy and nutritional status, which plays an important role in maintaining redox homeostasis and cell survival.<sup>26</sup> Some literatures have shown that the activation state of AMPK was negatively correlated with the occurrence of HCC.<sup>27</sup> AMPK can exert antitumor effects by complex crosstalk with many signal pathways,<sup>28</sup> such as the regulation of AMPK phosphorylation by Akt,<sup>29</sup> GSK3<sup>30</sup> and MEK-ERK.<sup>31</sup> Our results suggest that DMC not only directly affects the survival of tumor cells through AMPK pathway, but also regulates the stability of PD-L1 protein by enhancing AMPK $\alpha$  phosphorylation and binding to some amino acid sites on PD-L1 protein, thus reducing the overall immunosuppressive state of tumor microenvironment. It has been found that metformin can promote the direct binding of AMPK and PD-L1<sup>32–33</sup> and negatively affect the stability of PD-L1 to degrade it. Our data suggest that DMC may also be the embodiment of this mechanism.

At present, in the mechanism of drug inhibition of PD-1/PD-L1 signal pathway, except for the direct blocking effect of monoclonal antibody, most other compounds were related to the transcriptional level of genes. For example, bromodomain and extraterminal motif (BET) inhibitors trigger the transcriptional downregulation of CD274 by interrupting the direct interaction between BRD4 and CD274.<sup>34–35</sup> While HDAC6 inhibitors indirectly inhibit the transcription of CD274 through ARID1A.<sup>36</sup> PD-L1 is a highly glycosylated protein, and its polysaccharide structure plays a key role in the interaction between PD-L1 and PD-1.<sup>37–38</sup> Our mass spectrometric analysis and immunoprecipitation experiments showed that the inhibition of PD-L1 expression by DMC was related to ubiquitin degradation caused by abnormal protein processing, and it was realized by E3 ligase RBX1. The

regulation of PD-L1 expression by DMC was reflected at the protein level (inhibiting the normal synthesis of PD-L1 and promoting its ubiquitin degradation), indicating that small molecular compounds can show more diverse endogenous mechanisms.

Previous studies have shown that COX inhibitors combined with PD-1/PD-L1 antibodies can well enhance the immune response.<sup>19–39</sup> Considering that mPGES-1 inhibitors can avoid the serious side effects of COX inhibitors, we think that DMC combined with immunosuppression (PD-L1), but also provides an important strategic reference for multitarget or combined immunotherapy of HBV-related HCC.

**Funding** This study was supported by the Joint Funds for the Innovation of Science and Technology, Fujian province (2017Y9100), the Natural Science Foundation of Fujian Province (2018J01296), the Medical Innovation Project of Fujian Province (2017-CX-19), the Startup Fund for Scientific Research of Fujian Medical University (2017XQ2022), the National Natural Science Foundation of China (81470872) and the Construction Project of the Fujian Province Minimally Invasive Medical Center (No.[2017]171).

**Competing interests** None declared.

**Patient consent for publication** Not required.

**Ethics approval** The study was approved by the Research Ethics Review Committee of Fujian Medical University Union Hospital. All animals procedures were approved by the Animal Ethics Committee of Fujian Medical University and followed all animal care and use guidelines.

**Provenance and peer review** Not commissioned; externally peer reviewed.

**Data availability statement** Data are available upon reasonable request. All data relevant to the study are included in the article or uploaded as online supplementary information. Most data relevant to the study are included in the article or uploaded as supplementary information. Due to the excessive amount of microarray chip analysis and LC-MS/MS analysis, the data are available on reasonable request.

**Open access** This is an open access article distributed in accordance with the Creative Commons Attribution Non Commercial (CC BY-NC 4.0) license, which permits others to distribute, remix, adapt, build upon this work non-commercially, and license their derivative works on different terms, provided the original work is properly cited, appropriate credit is given, any changes made indicated, and the use is non-commercial. See <http://creativecommons.org/licenses/by-nc/4.0/>.

**ORCID iD**

Nanhong Tang <http://orcid.org/0000-0002-3960-4018>

## REFERENCES

- 1 Isogawa M, Tanaka Y. Immunobiology of hepatitis B virus infection. *Hepatol Res* 2015;45:179–89.
- 2 Lim CJ, Lee YH, Pan L, *et al*. Multidimensional analyses reveal distinct immune microenvironment in hepatitis B virus-related hepatocellular carcinoma. *Gut* 2019;68:916–27.
- 3 Ye B, Liu X, Li X, *et al*. T-Cell exhaustion in chronic hepatitis B infection: current knowledge and clinical significance. *Cell Death Dis* 2015;6:e1694.



- 4 Kahan SM, Wherry EJ, Zajac AJ. T cell exhaustion during persistent viral infections. *Virology* 2015;479-480:180-93.
- 5 Shire NJ. Cure strategies for hepatitis B virus: the promise of immunotherapy. *Clin Pharmacol Drug Dev* 2017;6:186-94.
- 6 Pardoll DM. The blockade of immune checkpoints in cancer immunotherapy. *Nat Rev Cancer* 2012;12:252-64.
- 7 Naidoo J, Page DB, Li BT, et al. Toxicities of the anti-PD-1 and anti-PD-L1 immune checkpoint antibodies. *Ann Oncol* 2016;27:1362.
- 8 Pei Y, Wang C, Yan SF, et al. Past, current, and future developments of therapeutic agents for treatment of chronic hepatitis B virus infection. *J Med Chem* 2017;60:6461-79.
- 9 Kalinski P. Regulation of immune responses by prostaglandin E2. *J Immunol* 2012;188:21-8.
- 10 Chou JP, Ramirez CM, Ryba DM, et al. Prostaglandin E2 promotes features of replicative senescence in chronically activated human CD8+ T cells. *PLoS One* 2014;9:e99432.
- 11 Xu Y, Zhao W, Xu J, et al. Activated hepatic stellate cells promote liver cancer by induction of myeloid-derived suppressor cells through cyclooxygenase-2. *Oncotarget* 2016;7:8866-78.
- 12 Chen Z, Cai X, Li M, et al. CRISPR/Cas9-based liver-derived reporter cells for screening of mPGES-1 inhibitors. *J Enzyme Inhib Med Chem* 2019;34:799-807.
- 13 Breinig M, Rieker R, Eiteneuer E, et al. Differential expression of E-prostanoid receptors in human hepatocellular carcinoma. *Int J Cancer* 2008;122:547-57.
- 14 Lu D, Han C, Wu T. Microsomal prostaglandin E synthase-1 promotes hepatocarcinogenesis through activation of a novel EGR1/ $\beta$ -catenin signaling axis. *Oncogene* 2012;31:842-57.
- 15 Chen S, Liu C, Wang X, et al. 15-Deoxy- $\Delta$ (12,14)-prostaglandin J2 (15d-PGJ2) promotes apoptosis of HBx-positive liver cells. *Chem Biol Interact* 2014;214:26-32.
- 16 Liu C, Chen S, Wang X, et al. 15d-PGJ<sub>2</sub> decreases PGE<sub>2</sub> synthesis in HBx-positive liver cells by interfering EGR1 binding to mPGES-1 promoter. *Biochem Pharmacol* 2014;91:337-47.
- 17 Zhang B, Yan Y, Li Y, et al. Dimethyl celecoxib sensitizes gastric cancer cells to ABT-737 via AIF nuclear translocation. *J Cell Mol Med* 2016;20:2148-59.
- 18 Egashira I, Takahashi-Yanaga F, Nishida R, et al. Celecoxib and 2,5-dimethylcelecoxib inhibit intestinal cancer growth by suppressing the Wnt/ $\beta$ -catenin signaling pathway. *Cancer Sci* 2017;108:108-15.
- 19 Sajiki Y, Konnai S, Okagawa T, et al. Prostaglandin E<sub>2</sub>-Induced Immune Exhaustion and Enhancement of Antiviral Effects by Anti-PD-L1 Antibody Combined with COX-2 Inhibitor in Bovine Leukemia Virus Infection. *J Immunol* 2019;203:1313-24.
- 20 Chen Y, Tian Z. HBV-Induced immune imbalance in the development of HCC. *Front Immunol* 2019;10:10.
- 21 Xie Y, Liu Y-K, Guo Z-P, et al. RBX1 prompts degradation of EXO1 to limit the homologous recombination pathway of DNA double-strand break repair in G1 phase. *Cell Death Differ* 2020;27:1383-97.
- 22 Wu S, Yang C, Guo S, et al. Stimulation of B7-H1 in hepatocarcinoma cells by hepatitis B virus X antigen. *Immunol Invest* 2010;39:754-69.
- 23 Sun Y, Yu M, Qu M, et al. Hepatitis B virus-triggered PTEN/ $\beta$ -catenin/c-Myc signaling enhances PD-L1 expression to promote immune evasion. *Am J Physiol Gastrointest Liver Physiol* 2020;318:G162-73.
- 24 Komohara Y, Fujiwara Y, Ohnishi K, et al. Tumor-Associated macrophages: potential therapeutic targets for anti-cancer therapy. *Adv Drug Deliv Rev* 2016;99:180-5.
- 25 Chen Y, Song Y, Du W, et al. Tumor-Associated macrophages: an accomplice in solid tumor progression. *J Biomed Sci* 2019;26:78.
- 26 Ren Y, Shen H-M. Critical role of AMPK in redox regulation under glucose starvation. *Redox Biol* 2019;25:101154.
- 27 Yang X, Liu Y, Li M, et al. Predictive and preventive significance of AMPK activation on hepatocarcinogenesis in patients with liver cirrhosis. *Cell Death Dis* 2018;9:264.
- 28 Hardie DG. AMPK--sensing energy while talking to other signaling pathways. *Cell Metab* 2014;20:939-52.
- 29 Hawley SA, Ross FA, Gowans GJ, et al. Phosphorylation by Akt within the ST loop of AMPK- $\alpha$ 1 down-regulates its activation in tumour cells. *Biochem J* 2014;459:275-87.
- 30 Suzuki T, Bridges D, Nakada D, et al. Inhibition of AMPK catabolic action by GSK3. *Mol Cell* 2013;50:407-19.
- 31 Shen C-H, Yuan P, Perez-Lorenzo R, et al. Phosphorylation of BRAF by AMPK impairs BRAF-KSR1 association and cell proliferation. *Mol Cell* 2013;52:161-72.
- 32 Cha J-H, Yang W-H, Xia W, et al. Metformin promotes antitumor immunity via endoplasmic-reticulum-associated degradation of PD-L1. *Mol Cell* 2018;71:606-20.
- 33 Xue J, Li L, Li N, et al. Metformin suppresses cancer cell growth in endometrial carcinoma by inhibiting PD-L1. *Eur J Pharmacol* 2019;859:172541.
- 34 Hogg SJ, Vervoort SJ, Deswal S, et al. BET-Bromodomain inhibitors engage the host immune system and regulate expression of the immune checkpoint ligand PD-L1. *Cell Rep* 2017;18:2162-74.
- 35 Zhu H, Bengsch F, Svoronos N, et al. Bet bromodomain inhibition promotes anti-tumor immunity by suppressing PD-L1 expression. *Cell Rep* 2016;16:2829-37.
- 36 Fukumoto T, Fatkhutdinov N, Zundell JA, et al. Hdac6 inhibition synergizes with anti-PD-L1 therapy in ARID1A-Inactivated ovarian cancer. *Cancer Res* 2019;79:5482-9.
- 37 Li C-W, Lim S-O, Chung EM, et al. Eradication of triple-negative breast cancer cells by targeting glycosylated PD-L1. *Cancer Cell* 2018;33:187-201.
- 38 Lee H-H, Wang Y-N, Xia W, et al. Removal of N-linked glycosylation enhances PD-L1 detection and predicts anti-PD-1/PD-L1 therapeutic efficacy. *Cancer Cell* 2019;36:168-78.
- 39 Zelenay S, van der Veen AG, Böttcher JP, et al. Cyclooxygenase-Dependent tumor growth through evasion of immunity. *Cell* 2015;162:1257-70.
- 40 Prima V, Kaliberova LN, Kaliberov S, et al. COX2/mPGES1/PGE2 pathway regulates PD-L1 expression in tumor-associated macrophages and myeloid-derived suppressor cells. *Proc Natl Acad Sci U S A* 2017;114:1117-22.
- 41 Patel SA, Minn AJ. Combination cancer therapy with immune checkpoint blockade: mechanisms and strategies. *Immunity* 2018;48:417-33.
- 42 Moslehi JJ, Salem J-E, Sosman JA, et al. Increased reporting of fatal immune checkpoint inhibitor-associated myocarditis. *Lancet* 2018;391:933.